BIOORGANIC CHEMISTRY **25,** 179–202 (1997)
ARTICLE NO. BH971065

Model Insect Cuticle Sclerotization: Reactions of Catecholamine Quinones with the Nitrogen-Centered Nucleophiles Imidazole and *N*-Acetylhistidine

Xin Huang,* Rongda Xu,† M. Dale Hawley,* and Karl J. Kramer‡

*Department of Chemistry and †Department of Entomology, Kansas State University, Manhattan, Kansas 66506; and ‡Grain Marketing and Production Research Center, Agricultural Research Service, United States Department of Agriculture,[1] Manhattan, Kansas 66502

Received March 24, 1997

The catecholamines *N*-acetyldopamine (NADA) and *N*-β-alanyldopamine (NBAD) are two precursors for quinonoios used as sclerotizing agents in insect cuticle. This study focused on the reaction pathways of the quinones of NADA and NBAD by using two nitrogen-centered nucleophiles, imidazole and *N*-acetylhistidine, to model cuticular proteins containing histidyl residues. The quinones were prepared by electrochemical oxidation, using either a coulometric microcell or a flow-through cell. The reactions of the quinones with the nucleophiles were investigated at physiological pH using electrochemical, chromatographic, and spectroscopic methods. The major products were purified by semipreparative liquid chromatography and identified by mass spectrometry and nuclear magnetic resonance spectroscopy to be nucleophilic addition products of the quinones with the nucleophiles bonded to two carbons in the aromatic ring. The predominant products for both nucleophiles were C6 adducts of NADA and NBAD. C2 adducts of *N*-acetylhistidine were minor products.

INTRODUCTION

Insect cuticle sclerotization or hardening is a vital process required for the survival of insects (*1–4*). During sclerotization, the chemical and mechanical properties and the appearance of the cuticle are changed: the water content decreases, the matrix proteins become much more resistant to extraction and degradation, and the cuticle becomes stiff and hard. This process has been under extensive study for several decades and especially so in recent years. In a recent model for the insect sclerotization process, catechols are first oxidized to their corresponding electrophilic *o*-quinones by cuticular phenoloxidases (*1*, *5*). The *o*-quinones are subsequently isomerized, first to *p*-quinone methides by quinone isomerases and then to α,β-dehydrocatechols by quinone methide isomerases. The α,β-dehydrocatechols are then oxidized to form the corresponding dehydrocatechol *o*-quinones, which are subsequently isomerized into *p*-quinone methides. All these quinonoid intermedi-

[1] The Agricultural Research Service, USDA, is an equal opportunity/affirmative action employer and all agency services are available without discrimination.

0045-2068/97 $25.00

ates can act as sclerotizing agents and react directly with nucleophilic groups of cuticular proteins to form covalent bonds. The three different pathways involving reactions of nucleophiles with quinones, quinone methides, and α,β-dehydrocatechols are denoted as quinone tanning, quinone methide sclerotization, and α,β-sclerotization, respectively (*1*, *6*, *7*). The protein-bonded catechols, then, might be oxidized again and form another round of sclerotizing agents, which can react with nucleophilic groups in other protein molecules. This second addition results in covalent cross-linking between polypeptide chains via aromatic or side-chain carbons of catechols. In addition to these covalent cross-links, replacement of water in cuticle with catechols or their polymeric oxidation products and formation of numerous noncovalent interactions might also further stabilize the protein–chitin matrix of the cuticle (*1*, *8*).

Catechols that act as immediate precursors for quinonoid-sclerotizing agents in insect cuticle are primarily *N*-acyl derivatives of dopamine, such as *N*-acetyldopamine (NADA)[2] and *N*-β-alanyldopamine (NBAD) (*1*). Although other catechols, for example, 3,4-dihydroxyphenylalanine, 3,4-dihydroxyphenylacetic acid, *N*-acetylnorepinephrine, and *N*-β-alanylnorepinephrine, have also been detected in extracts of insect cuticles, their roles in sclerotization are less certain (*2*). Until now, convincing evidence for precursor roles was available only for NADA and NBAD. NADA was found to be present in several insect species in 1962 and has been demonstrated to be incorporated into cuticle during the sclerotization process (*9*, *10*). In 1982, NBAD was discovered to be a major precursor for tanning agents in stiff brown cuticles (*11*, *12*). Although the involvement of NADA and NBAD in sclerotization has been established, the mechanisms (Scheme 1) by which these compounds serve as precursors for quinonoios used as sclerotizing agents have not been fully elucidated and some aspects remain controversial.

The nucleophilic groups of cuticular proteins that react with the quinonoid agents have been suggested to be α-amino groups, ε-amino groups of lysyl residues, and imidazole nitrogens of histidyl residues (*1*, *13*). Other nucleophilic groups of cuticular proteins, such as thiol, hydroxyl, and carboxyl groups, might participate in cross-linking as well, but their involvement is probably minor (*1*). Direct evidence for the existence of covalent bonds between catecholamines and nucleophilic groups in cuticular proteins had not been obtained until solid-state nuclear magnetic resonance (NMR) was used to examine the C–N covalent linkages in the pupal cuticle of the tobacco hornworm (*14–17*). It was determined by double cross-polarization magic-angle-spinning ^{13}C NMR that the histidyl nitrogens of cuticular protein were attached to aromatic ring carbons of a catecholamine in pupal exuviae prepared from *Manduca sexta* larvae injected with both [1,3-$^{15}N_2$]histidine and [ring-$^{13}C_6$]dopamine

[2] Abbreviations used: NADA, *N*-acetyldopamine; NBAD, *N*-β-alanyldopamine; NMR, nuclear magnetic resonance spectroscopy; NAcH, *N*-acetylhistidine; DA, dopamine; DMF, *N*,*N*-dimethylformamide; MS, mass spectrometry; LC, liquid chromatography; MALDI-MS, matrix-assisted laser desorption mass spectrometry; EC, electrochemical detection; 6-Imid-NADA, 6-(*N*-imidazole)-*N*-acetyldopamine; 6-Imid-NBAD, 6-(*N*-imidazole)-*N*-β-alanyldopamine; HMQC, heteronuclear multiple quantum coherence; TOCSY, total correlation spectroscopy; 6-NAcH-NADA, 6-(*N*-acetylhistidyl)-*N*-acetyldopamine; 2-NAcH-NADA, 2-(*N*-acetylhistidyl)-*N*-acetyldopamine; 6-NAcH-NBAD, 6-(*N*-acetylhistidyl)-*N*-β-alanyldopamine; 2-NAcH-NBAD; 2-(*N*-acetylhistidyl)-*N*-β-alanyldopamine.

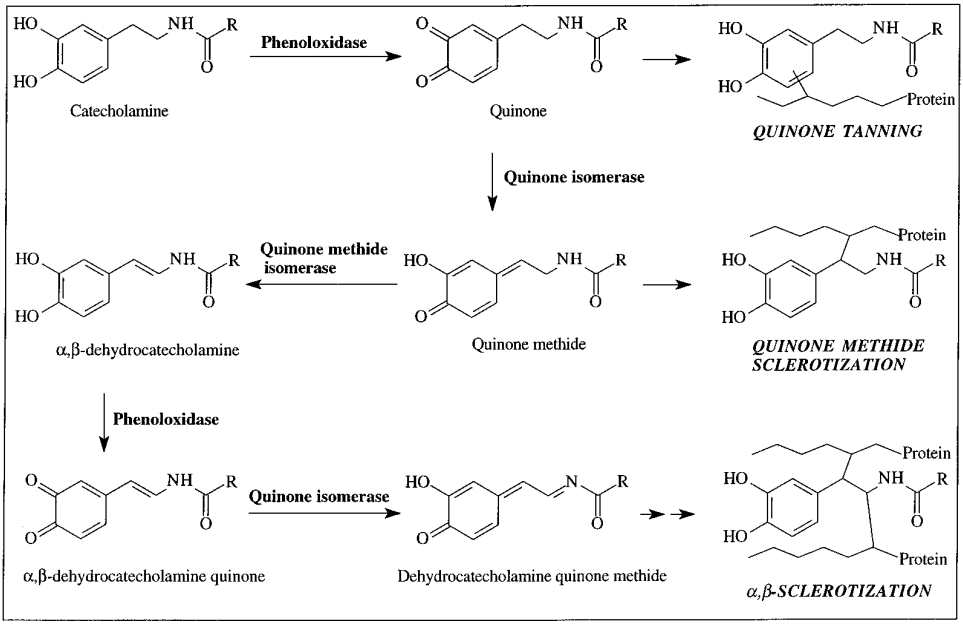

SCHEME 1

(*14*). In addition, a linkage between a histidyl nitrogen and the β-carbon in the side-chain of catechols in the pupal exuviae from larvae that had been injected with both [1,3-$^{15}N_2$]histidine and [β-$^{13}C_6$]dopamine was found by rotational echo double resonance ^{13}C NMR (*15*). The results of these solid-state NMR studies are consistent with a sclerotization mechanism in which quinones and quinone methides derived from *N*-acylcatecholamines form covalent bonds with functional groups of cuticular proteins. However, the exact structures of the histidyl-catechol ring or side-chain carbon addition adducts could not be determined by the solid-state NMR studies.

In vitro evidence for cuticle-catalyzed formation of adducts between NADA and amino acid derivatives was obtained from the analysis of products derived from their incubation with cuticle or cuticular enzymes (*18–21*). The structures of a few of these model adducts have also been determined. Recently, four histidyldopamine adducts were isolated and characterized from an acid hydrolysate of *M. sexta* pupal cuticle (*22*). These adducts apparently are formed from Michael 1,4- and 1,6-addition reactions with quinonoios used as sclerotizing agents. Thus, the imidazole side chain of histidine residues in cuticular proteins are nucleophiles critical for sclerotization.

Although knowledge about the chemistry of cuticular sclerotization has increased substantially in recent years, many aspects are still unclear. For example, the identities of most quinonoios used as sclerotizing agents and products have not been directly established and the kinetics of the reactions between the sclerotizing agents and functional groups of proteins have not been determined. The objective of this

study was to elucidate the reaction pathways of the quinones of the catecholamines NADA and NBAD, which are immediate precursors for sclerotizing agents in insect cuticle, by using amino acid derivatives to model the functional groups in cuticular protein. Two nitrogen-centered nucleophiles, imidazole and *N*-acetylhistidine (NAcH), were employed.

EXPERIMENTAL

Syntheses of Catecholamines

Although some NADA was obtained commercially (Sigma Chemical Co., St. Louis, MO),[3] most was synthesized from dopamine (DA) using a procedure modified from that of Andersen (*23*). First, 0.80 g DA hydrochloride (Sigma Chemical Co.) was dissolved in 40 ml of 10% potassium tetraborate that had been purged with nitrogen. Then, 0.44 ml of 99% acetic anhydride (Fisher Scientific Co., Pittsburgh, PA) was slowly added over a period of 30 min to the DA hydrochloride solution under a nitrogen atmosphere. To verify the completeness of the acetylation reaction, 1-μl aliquots of the product mixture were subjected to thin-layer chromatography on silica gel sheets (Eastman Kodak Co., Rochester, NY) using methanol as the developing solvent. The retention factors of DA and NADA were 0.40 and 0.83, respectively. After all DA had reacted, 2 ml of concentrated formic acid (Fisher Scientific Co., Pittsburgh, PA) were added to the product mixture to precipitate the boric acid. After filtration through Whatman No. 1 paper, the supernatant was subjected to gel filtration chromatography on a column packed with Bio-Gel P-2 (Bio-Rad Laboratories, Richmond, CA) using 0.02% formic acid as the mobile phase. The effluent was monitored spectroscopically at a wavelength of 280 nm. Fractions were collected and analyzed by analytical liquid chromatography (LC) for the presence of NADA. Those fractions showing only NADA were pooled and lyophilized. NADA was obtained as a white powder in 80% overall yield. Mass spectrometry (MS), NMR, and LC analyses confirmed that the desired product had been prepared.

NBAD was synthesized from DA using a method modified from Kramer *et al.* (*24*) and Yamasaki *et al.* (*25*). First, 0.96 g DA hydrochloride was dissolved in 17.5 ml *N*,*N*-dimethylformamide (DMF) (Fisher Scientific Co., Pittsburgh, PA) that had been deaerated with nitrogen and predried with molecular sieves (size: 5 Å). The molecular sieves had been activated by heating at 600°C for a period of 24 h in the stream of nitrogen. *N*-Methylmorpholine (0.55 ml) (Sigma Chemical Co.) and *N*-*t*-butyloxycarbo-β-alanine-*N*-hydroxysuccinimide ester (17.2 g) (Chemalog, Chemical Dynamics Co., NJ) were dissolved in a second 17.5-ml volume of DMF. The two DMF solutions were combined and stirred for 48 h under a nitrogen atmosphere in an ice water bath. 1-(2-Aminoethyl)piperazine (0.26 ml) (Aldrich Chemical Co., St. Louis, MO) was then added to the product mixture in an ice water bath, after which the solution was allowed to warm to room temperature.

[3] Mention of a proprietary product does not constitute a recommendation by the USDA.

Another 0.52 ml of 1-(2-aminoethyl)piperazine was added to the mixture, which was then stirred for another hour. The product mixture was acidified with 100 ml of 0.25 M H_2SO_4 and extracted with 100 ml of ethyl acetate. Extraction of the aqueous layer with 30 ml of ethyl acetate was repeated three times. The extracts were subsequently pooled, washed with saturated NaCl solution three times, and dried over sodium sulfate under nitrogen overnight. The ethyl acetate extract was then filtered through Whatman paper and reduced to a volume of about 10 ml using a rotary evaporator, at which time a white solid formed. The suspension was filtered and the solid was collected and allowed to dry under vacuum for about 4 h. The dried solid was dissolved in 4 ml of a HCl : 1,4-dioxane (1 : 2) solution and left at room temperature for 3 h. The solution was reduced to a small volume using a rotary evaporator. Diethyl ether was added to the concentrated solution in sufficient volume to ensure precipitation of NBAD · HCl, which was collected by filtration, washed with diethyl ether, and dried under vacuum overnight. The yield was 68% (0.90 g). MS and NMR analyses confirmed that the desired product had been prepared.

Preparation of Catecholamine Quinones

Electrochemical oxidation was used to prepare the quinones. If chemical oxidation were to be used to prepare quinones, excess oxidizing agents would be generally employed to ensure complete oxidation of the catecholamines. However, if quinones thus obtained were to react with nucleophiles directly and form adducts, then the presence of the excess oxidizing agent might cause complications by oxidizing the adducts. In contrast, the electrochemical oxidation method results in the preparation of quinones that are devoid of excess oxidizing agent.

Since the quinones are relatively stable at low pH, the electrosynthesis of the quinones was conducted at pH 2.0 in the absence of nucleophiles. The supporting electrolyte was 0.01 N HCl and 0.09 N KCl. The potential for oxidation of NADA or NBAD was controlled at 0.7 V vs Ag/AgCl (saturated KCl). A custom-made, three-electrode coulometer (*26*) was used to apply a constant potential for electrolysis and to give instantaneous digital coulomb and analog current readouts. A Hewlett–Packard (Palo Alto, CA) 3390A integrator was used to monitor the electrolysis current. Either a coulometric microcell or a coulometric flow-through cell was used for the oxidation.

Coulometric microcell. A coulometric microcell was designed to prepare small quantities of quinones (Fig. 1) (*27*). Volumes of catecholamine solutions used for each batch preparation ranged from 0.4 to 1.5 ml. The large surface area to volume ratio of the working electrode and efficient mixing of the solutions permit rapid and quantitative coulometric conversion. Separation of the auxiliary and working electrodes by the membrane filter prevents mixing of the anode and cathode products, thereby permitting complete electrolysis. The close proximity of the reference electrode to the working electrode minimizes uncompensated iR drop and allows accurate control of the potential under high-current conditions. In addition, the small volume of the sample compartment and short electrolysis time make the cell suitable for use when starting materials are available in

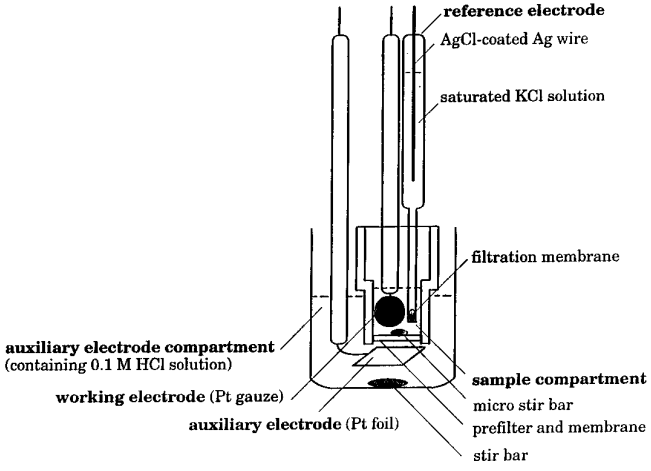

FIG. 1. Diagram of the microelectrochemical cell. The sample compartment is a polypropylene tube containing a prefilter and a 0.2-μm-pore size nylon 66 membrane at the tip. The working electrode is a piece of platinum gauze (20 $\times$ 50 mm) that was folded and shaped into a small sphere (diameter, ~5 mm). The reference electrode is a AgCl-coated silver wire placed inside a glass tube containing a saturated KCl solution; a 0.2-μm-pore size filtration membrane was used as the divider and sealed inside the tube tip. The auxiliary electrode is a platinum foil (5 $\times$ 10 mm). The stir bars in the sample compartment and the auxiliary electrode compartment are 5 and 20 mm, respectively.

limited quantity and/or when relatively reactive compounds are to be synthesized. This microcell was used for the electrosyntheses of reactive quinones that were immediately used for kinetics studies and subsequent reactions with nucleophiles.

Flow-through coulometric cell. To synthesize sufficient quantities of catecholamine–nucleophile adducts for structural analysis and characterization, relatively large-scale electrosyntheses of catecholamine quinones were required. Since catecholamine quinones are reactive, batch preparation is not desirable when a long electrolysis time is required. Hence, a flow-through coulometric cell was constructed that permits electrolysis of a relatively large amount of catecholamine and allows the quinone to react with a nucleophile shortly after formation of the quinone (Fig. 2) (*27*). Catecholamine solutions were introduced from a sample reservoir by gravity flow into the sample compartment and were electrolyzed to form quinones at a controlled potential (0.8 V). The quinone effluent was added to a stirred solution of the nucleophile to form adducts at pH 7.0. In this flow-through cell, rapid and efficient coulometric conversion was achieved with a large ratio of working electrode surface area to solution volume, a concentric arrangement of the working and the auxiliary electrodes, and a nylon membrane that separated the working and the auxiliary electrode compartments. Both a low uncompensated iR drop and accurate potential control were the result of the close proximity of the tip of the reference electrode to the working electrode. The cell design allowed the catecholamine quinones to react with nucleophiles

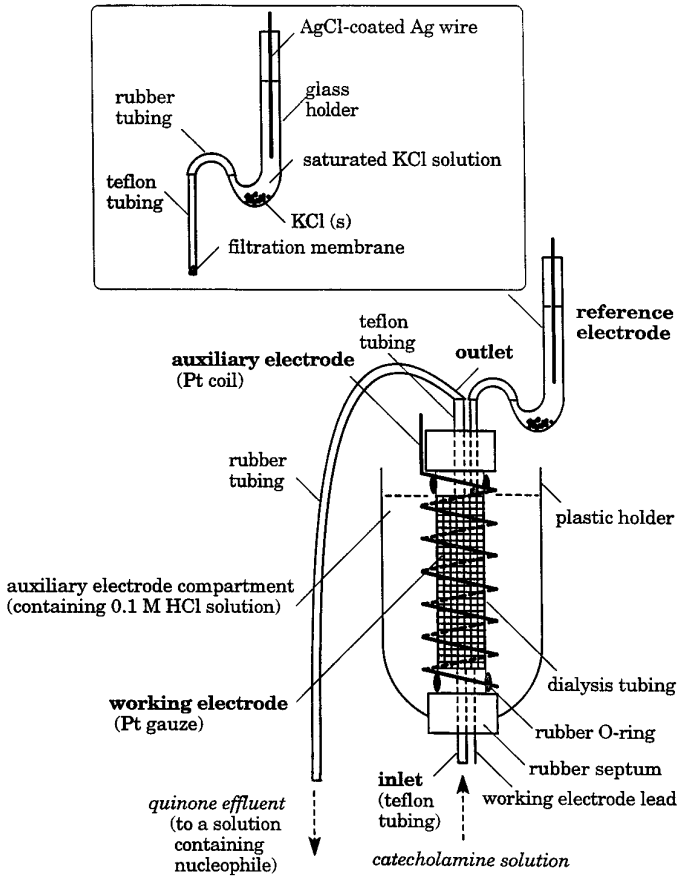

FIG. 2. Diagram of the flow-through electrochemical cell. The working electrode is a platinum gauze that was tightly folded and placed in the cellulose dialysis tubing. Rubber septa were inserted into both ends of the dialysis tubing. A tight seal between the dialysis tubing and the rubber septa was attained by addition of rubber o-rings that encircled the ends of the dialysis tubing. The Teflon tubing tip of the reference electrode was inserted into the dialysis tubing and positioned close to the upper portion of working electrode. The auxiliary electrode encircled the dialysis tubing. The auxiliary electrode compartment contained about 4.5 ml of 0.1 M HCl solution. Solutions were introduced by gravity flow into the dialysis tubing. The direction of fluid flow was from the bottom to the top of the cell. The dead volume of the sample compartment in the dialysis tubing was about 0.3 ml.

outside of the cell almost immediately after their formation. This minimizes quinone decay, which might occur during long-term electrolysis of a large quantity of catecholamines in a batch cell. It also precludes electrochemical oxidation of adducts that would have occurred if the catecholamine were electrolyzed in the presence of nucleophiles. This cell is efficient for relatively large-scale electrochemical syntheses and is especially useful when the electrogenerated intermediates are highly reactive and must be mixed with other substrates shortly after their formation to produce the desired products.

Syntheses of Catecholamine Adducts

Catecholamine adducts were synthesized at pH 7 by adding the effluent from the flow-through coulometric cell, which contained NADA or NBAD quinone at pH 2, into a solution of a nucleophile (*vide supra*). Purification of adducts formed in the reaction mixtures was carried out using either gel filtration or semipreparative LC.

Gel filtration of the product mixtures from the reactions of quinones and imidazole was performed using a column packed with Bio-Gel P-2 (Bio-Rad Laboratories). The mobile phase used was 0.05% formic acid. The effluent containing an adduct in dilute formic acid was lyophilized to yield the adduct as a white solid.

Purification using semipreparative LC was performed as described previously (*28*). A binary mobile phase system was used that consisted of solvents A and B. Solvent A was 150 mM formic acid and 30 mM ammonium formate (pH 3.0), whereas solvent B was 50% methanol (uv cutoff: 204 nm), 180 mM formic acid, and 8 mM ammonium formate (pH 3.0). For adducts of NBAD quinone with NAcH, the gradient employed was 0–15 min, 100% solvent A; and 15–30 min, linear gradient from 0 to 50% solvent B.

Analytical Liquid Chromatography

Analytical LC was conducted to analyze the compositions of product mixtures. The liquid chromatography system and the uv/vis and electrochemical detectors were the same as those used previously (*28*). Separation was achieved on a Microsorb-MV C18 stainless steel column (5 μm, 4.6 $\times$ 250 mm) (Rainin Instrument Co., Inc., Woburn, MA) using a flow rate of 1 ml/min. As was reported previously, during LC analysis of quinones, stainless steel in the columns, including the inlet and outlet frits, causes on-column reduction of quinones, which might lead to misidentification of chromatographic peaks (*29*). In the current LC studies of product mixtures from reactions of quinones with nucleophiles, samples were injected into columns after the quinones had been completely consumed by nucleophiles. Thus, on-column reduction of quinones was not a concern.

The binary mobile phase system, which consisted of solvents A and B, was used (see the preceding section). For the product mixtures produced from NADA quinone reacting with imidazole, the gradient was 0–15 min, 80% solvent A and 20% solvent B; and 15–30 min, linear gradient from 20 to 80% solvent B. For the product mixtures from the reaction of NBAD quinone with imidazole, the gradient was 0 min, 90% solvent A and 10% solvent B; 0–15 min, linear gradient from 10 to 14% solvent B; 15–20 min, linear gradient from 14 to 25% solvent B; and 20–25 min, linear gradient from 25 to 40% solvent B. For the product mixtures from NBAD quinone reacting with NAcH, the gradient was 0 min, 100% solvent A; 0–20 min, linear gradient from 0 to 20% solvent B; and 20–30 min, linear gradient from 20 to 30% solvent B.

UV/Vis Spectroscopy

In addition to on-line uv/vis detection conducted during analytical LC, uv/vis spectra of adducts in 0.01 M HCl solution and uv/vis spectral changes associated with reactions of NADA quinone or NBAD quinone with various nucleophiles

and/or in various buffers were recorded in a 1.0-cm quartz cuvette using a Hewlett–Packard (Palo Alto, CA) HP 8452A diode array spectrophotometer. For studies of reactions of quinones with nucleophiles, once electrolysis of varying concentrations of NADA or NBAD in 0.01 M HCl and 0.09 M KCl was completed, 0.195 ml of electrogenerated NADA quinone or NBAD quinone was added to 0.455 ml of either a nucleophile solution or a buffer in the quartz cuvette to give 0.650 ml of a 3 : 10 diluted quinone solution at the desired nucleophile or buffer concentration and pH. The uv/vis measurements within the wavelength range of 200 to 800 nm were initiated 15 s after mixing and conducted for 10 min at 15-s intervals. The cell temperature was controlled at 25°C by using a temperature-regulated circulating water bath.

The spectral data were used to estimate the initial rate constants for the reaction of NADA quinone or NBAD quinone with imidazole or *N*-acetylhistidine. To do this, the absorbance changes at 396 nm with time were extracted from each set of spectra. To compensate for instrument drift from one spectrum to the next, the absorbance at 396 nm was corrected by subtracting the absorbance at 700 nm, where there is no absorption from reactants or products. Regression analyses of log(corrected absorbance at 396 nm) vs time were performed to obtain the pseudo-first-order rate constants (Table 1). For the reaction between a quinone and nucleophile, the reaction rate law is expected to be

$$\text{reaction rate} = k[\text{quinone}][\text{nucleophile}] = k'[\text{quinone}]. \qquad [1]$$

Cyclic Voltammetry, Mass Spectrometry, and Nuclear Magnetic Resonance Spectroscopy

The cyclic voltammetry and NMR systems and conditions used were the same as described previously (*28*). Electrospray MS of adducts was carried out either at the National Institute of Environmental Health Sciences (Research Triangle Park, NC) or at the University of Kansas (Lawrence, KS). A few adducts were characterized by matrix-assisted laser desorption mass spectrometry (MALDI-MS) at Kansas State University.

RESULTS

Spectroscopic Studies of Reactions of N-Acetyldopamine and N-β-Alanyldopamine Quinones with Imidazole

The uv/vis spectroscopic studies of the kinetics of the reaction of NADA and NBAD quinones with imidazole were performed at various pH values and molar ratios. In all cases studied, the analytical concentration of imidazole was at least 10 times greater than that of the quinone, such that the kinetics behavior of the quinones was investigated under pseudo-first-order conditions.

The uv/vis spectra that were recorded for 0.3 mM NADA quinone in 200 mM

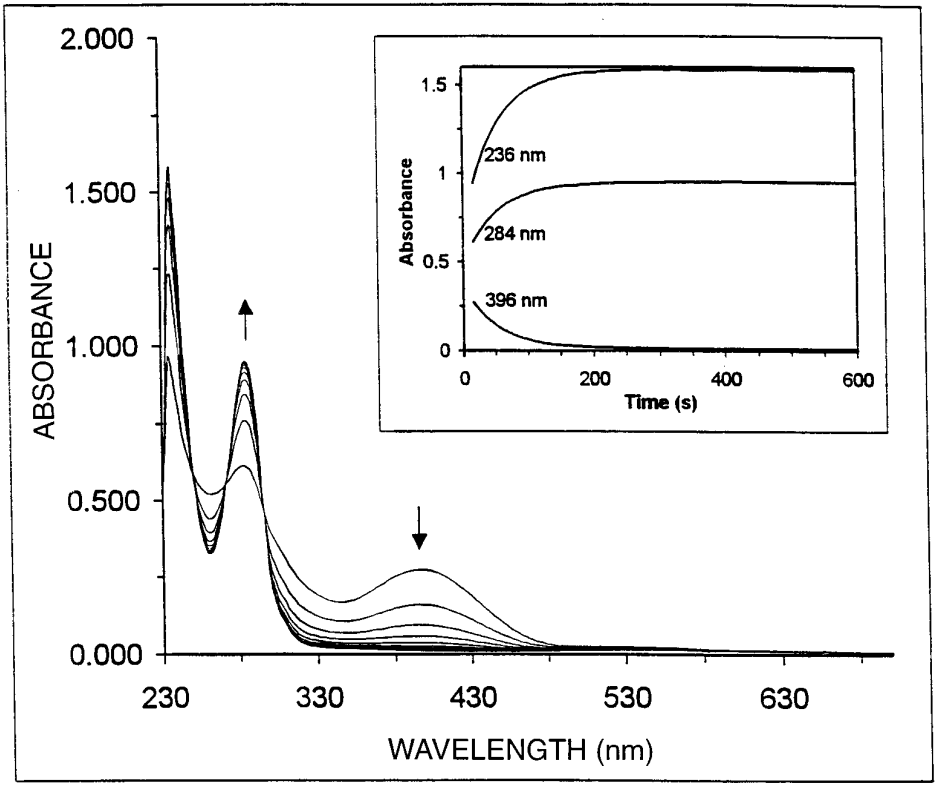

FIG. 3. Spectral changes associated with the reaction of 0.3 mM NADA quinone with 200 mM imidazole at pH 7.0. Although spectral measurements were conducted at 15-s intervals from 15 to 600 s after mixing of NADA quinone and imidazole solutions, for clarity only every other spectrum is shown here. (Inset) Absorbances at 236, 284, and 396 nm vs time.

imidazole at pH 7.0 are shown in Fig. 3, with three absorbance–time curves appearing as an inset. The absorbance at the λ_{max} of the quinone, 396 nm, decreases with time, indicating consumption of the quinone, whereas the absorbances at 236 and 284 nm increase, indicating the formation of a new product(s). The major product was determined to be an adduct of the corresponding catecholamine quinone with imidazole (*vide infra*). Similar changes in absorbances were also observed for quinones of various concentrations in the presence of various concentrations of imidazole and at different pH values. Comparable results were obtained for the kinetics behavior of NBAD quinone in the presence of imidazole (data not shown).

A broad absorption from ca. 300 to 600 nm is observed in the uv/vis spectra of some NBAD quinone reaction systems, such as in the case of 0.3 mM NBAD quinone in the presence of 50 mM imidazole at pH 7 (Fig. 4). This result indicates that another product(s) is forming in addition to the adduct of NBAD and imidazole. When the ratio of imidazole to NBAD quinone decreases or when the pH value

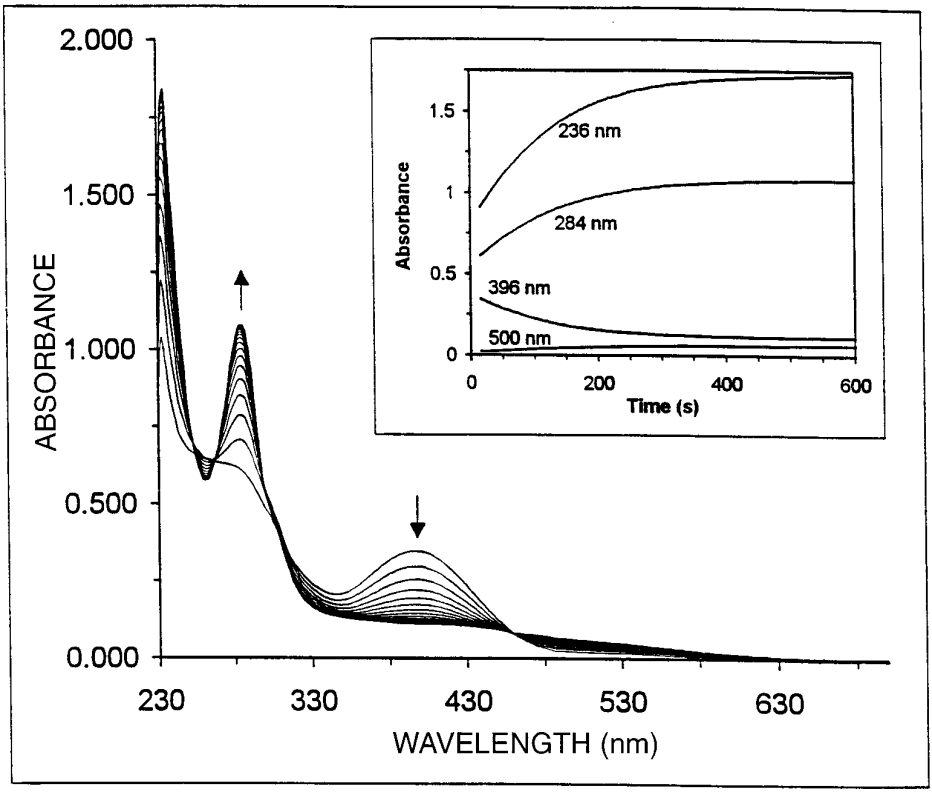

FIG. 4. Spectral changes associated with appearance of an unidentified species during the decay of 0.3 mM NBAD quinone in the presence of 50 mM imidazole at pH 7.0. Although spectral measurements were conducted at 15-s intervals from 15 to 600 s after mixing of NBAD quinone and imidazole solutions, for clarity only every other spectrum is shown here. The unidentified species has a broad absorption from ca. 300 to 600 nm. (Inset) Absorbances at 236, 284, 396, and 500 nm vs time.

increases, formation of the minor product becomes more evident (data not shown). A similar phenomenon also occurs for both NADA and NBAD quinones in buffer solutions in the absence of imidazole (unpublished data). Apparently, this phenomenon is due to a side reaction(s) of the quinones, which competes with the addition reaction of imidazole.

The effects of quinone concentrations, imidazole concentration, and pH on rate constants for the quinone reactions were examined and the expected rate law (Eq. [1]) was confirmed. First, the pseudo-first-order rate constants for reactions of 0.15, 0.3, 0.6, and 0.9 mM NADA quinone (Table 1) or NBAD quinone with 50 mM imidazole at pH 7.0 were found to be independent of the quinone concentration. Second, the pseudo-first-order rate constants for reactions of 0.3 mM NADA quinone (Table 1) or NBAD quinone with 20, 50, 100, and 200 mM imidazole at pH 7.0 showed the expected linear dependence on the concentration of imidazole.

TABLE 1
Rate Constants for NADA Quinone/Imidazole System

No.	[NADA quinone] (mM)	C_{Imid} (mM)[a]	pH	$[Imid]_{eq}$ (mM)[b]	Pseudo-first-order rate const.[c] (s^{-1}) × 10^3	Second-order rate const.[d] (M^{-1} s^{-1}) × 10^2
1	0.15	50	7.0	25	2.1	8.4
2	0.30	50	7.0	25	2.3	9.2
3	0.60	50	7.0	25	2.2	8.8
4	0.90	50	7.0	25	2.8	11
5	0.30	20	7.0	10	1.1	11
6	0.30	100	7.0	50	4.1	8.2
7	0.30	200	7.0	100	7.0	7.0
8	0.30	50	6.1	5.6	0.5	9.3
9	0.30	50	8.0	45.5	3.7	8.1

[a] C_{imid} is the analytical concentration of imidazole, i.e., the sum of the equilibrium concentrations of imidazole and its conjugate acid, imidazolium ion.

[b] $[Imid]_{eq}$, the equilibrium concentration of imidazole, is calculated using the corresponding analytical concentration and the pK_a of imidazolium ion, which is 7.0.

[c] The pseudo-first-order rate constants were obtained from slopes of plots for regression analyses of log(absorbance at 396 nm) vs time.

[d] The second-order rate constants were obtained by dividing the corresponding pseudo-first-order rate constants by the equilibrium concentrations of imidazole at the specified pH.

Third, the results obtained for reactions of 0.3 mM NADA quinone (Table 1) or NBAD quinone with 50 mM imidazole at pH 6.1, 7.0, and 8.0 show that pseudo-first-order rate constants increase with pH in this pH range. This is expected, since the fraction of imidazole that is not protonated increases with increasing pH. The pK_a of imidazolium ion is 7.0. At each pH, the equilibrium concentration of imidazole, i.e., the effective concentration of imidazole as a nucleophile was calculated from the corresponding analytical concentration of imidazole and the pK_a of imidazolium ion (Table 1). From the equilibrium concentration of imidazole and the pseudo-first-order rate constant (k'), the second-order rate constant for reaction of the quinone with the imidazole (k) was obtained by using $k = k'/[\text{Imidazole}]$ (Table 1). The average second-order rate constants are 9.0×10^{-2} M^{-1} s^{-1} for the reaction of NADA quinone with imidazole and 7.4×10^{-2} M^{-1} s^{-1} for the reaction of NBAD quinone with imidazole.

Liquid Chromatographic Studies of Product Mixtures from Reactions of N-Acetyldopamine and N-β-Alanyldopamine Quinones with Imidazole

The compositions of the product mixtures obtained from mixing 90 μl of 1 mM NADA quinone or NBAD quinone with 225 μl of 40 or 400 mM imidazole (1 : 100 or 1 : 1000 molar ratio) at pH 7.0 were analyzed by LC with uv/vis and electrochemical detection (EC) under different gradient conditions. LC-EC (reduction) chromatograms for product mixtures showed no discernible peaks (data not shown), which indicates that the quinone had been consumed completely. In the corresponding

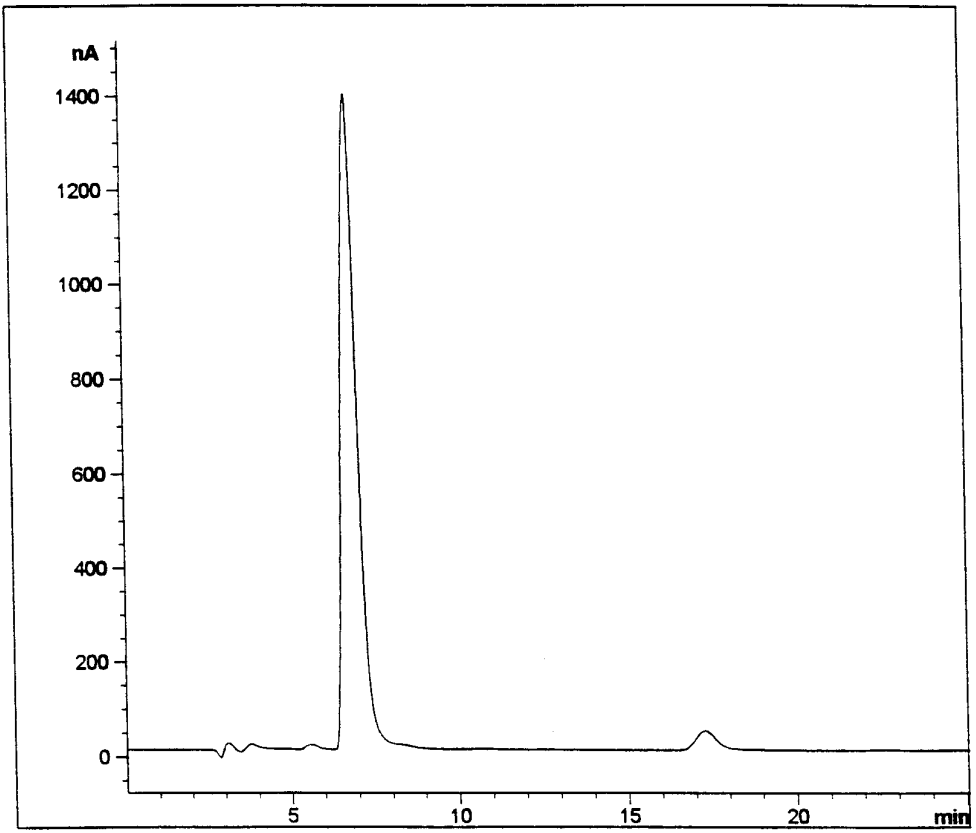

FIG. 5. LC-EC (oxidation) chromatogram of the product mixture from the reaction of NADA quinone with imidazole (1:1000 molar ratio) at pH 7.0.

LC-EC (oxidation) chromatograms for the products from reactions of NADA quinone with imidazole (Fig. 5), there is one major peak at 6.8 min and a minor peak at 17.4 min. The reaction product that gives rise to the peak at 6.8 min is denoted here as Imid-NADA. The peak at 17.4 min is due to NADA. For the product mixtures from reactions of NBAD quinone with imidazole, the LC-EC (oxidation) chromatograms obtained using a different gradient exhibit one major peak at 5.4 min and a minor peak at 12.7 min (data not shown). The peak at 5.4 min is due to reaction product, which is denoted as Imid–NBAD, whereas the peak at 12.7 min is due to NBAD.

The amounts of the adduct and the catecholamine produced in either the NADA quinone system or the NBAD quinone system were found to be dependent upon the molar ratio of the initial concentrations of the quinone and imidazole. The [Imid–NADA]:[NADA] ratios were approximately 4:1 and 26:1 when the [NADA quinone]:[imidazole] ratios were 1:100 and 1:1000, respectively. The

[Imid–NBAD] : [NBAD] ratios were 2 : 1 and 25 : 1 when [NBAD quinone] : [imidazole] ratios were 1 : 100 and 1 : 1000, respectively.

Identification and Characterization of Imidazole Adducts of N-Acetyldopamine and N-β-Alanyldopamine

In order to identify Imid–NADA and Imid–NBAD, the adducts were synthesized and purified for structural analysis and characterization. Their molecular masses were determined by electrospray MS. The former has MH^+ at $m/z = 262$ and the latter has MH^+ at $m/z = 291$. These m/z values are the same as the theoretical values for monoaddition adducts of imidazole with the corresponding quinones.

The structure of the Imid–NADA adduct was determined by ^1H NMR spectroscopic studies (data not shown). The ^1H spectrum shows two well-resolved singlets in the aromatic region at 6.81 and 6.64 ppm. This result indicates that neither *o*-coupling nor *m*-coupling occurs between these two protons. Hence, Imid–NADA must be the C6 mono-addition adduct, 6-*N*-imidazole-*N*-acetyldopamine (6-Imid–NADA). The chemical shift assignments for this adduct are as follows: δ (ppm) = 7.59 (s, 1H, H2′), 7.10 [s (br.), 1H, H5′], 7.02 (d, 1H, $J = 7.5$ Hz, H4′), 6.81 (s, 1H, H2), 6.64 (s, 1H, H5), 3.12 (t, 2H, $J = 7.5$ Hz, H8), 2.36 (t, 2H, $J = 7.5$ Hz, H7), 1.77 (s, 3H, H11) (see Scheme 2 for structure). The structure of Imid–NBAD was not determined, but it is assumed to be the C6 monoaddition adduct, 6-*N*-imidazole-*N*-β-alanyldopamine (6-Imid–NBAD).

The uv/vis spectra of 6-Imid–NADA and 6-Imid–NBAD, which were taken during LC of the product mixtures from the reactions of NADA quinone and NBAD quinone with imidazole, show that both adducts have a λ_{max} at 284 nm (data not shown).

Cyclic Voltammetric Studies of N-β-Alanyldopamine in the Presence of N-Acetylhistidine

The electrochemical behavior of NBAD in the presence of NAcH in 0.1 M phosphate buffer at pH 7.0 was studied at various molar ratios and scan rates. In the cyclic voltammogram obtained for 0.3 mM NBAD in the presence of 0.4 M NAcH at a scan rate of 100 mV/s, the first cycle of the voltammogram of NBAD consists of an anodic peak at 0.184 V and a cathodic peak at 0.134 V (Fig. 6). The anodic peak is due to the two-electron oxidation of NBAD to NBAD quinone and the cathodic peak is due to the reduction of the NBAD quinone to NBAD. On subsequent cycles another redox couple emerges at a potential that is 75 mV more positive than the anodic and cathodic peaks for the NBAD/NBAD quinone couple. The relative magnitudes of the new peaks increase with either increasing scan number or decreasing scan rate, whereas the relative peak heights for the NBAD/NBAD quinone couple decrease. These results indicate that NBAD quinone undergoes a relatively slow chemical reaction with NAcH under these conditions to give one or more products that are oxidized at more positive potentials. The rate of the reaction is too slow to be measured accurately by cyclic voltammetry.

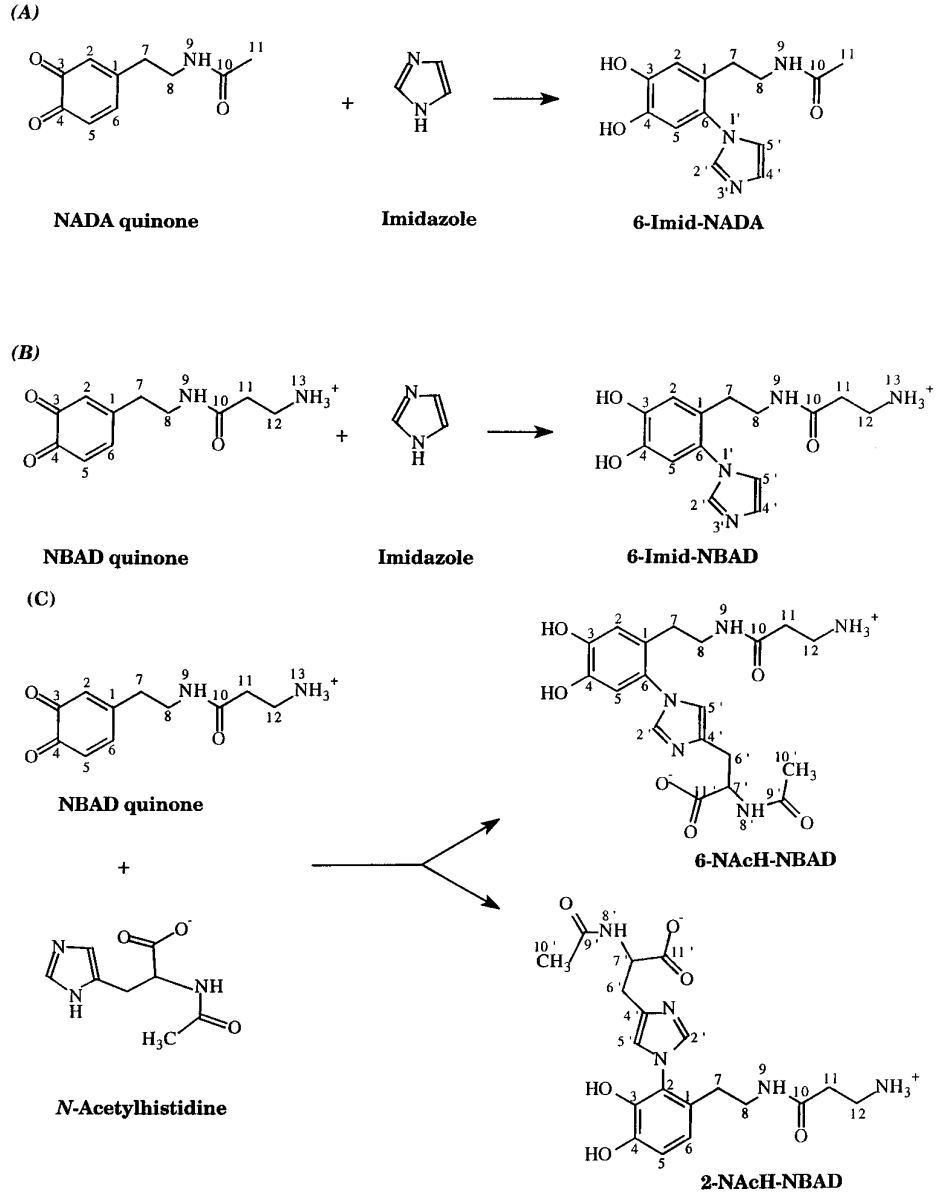

SCHEME 2

UV/Vis Spectroscopy of Reactions of N-β-Alanyldopamine Quinone with N-Acetylhistidine

Ultraviolet/visible spectroscopic studies of the kinetics of the reaction of NBAD quinone with NAcH solutions (pH 7.0) were also performed at different molar ratios under pseudo-first-order conditions. In the uv/vis spectra that were recorded

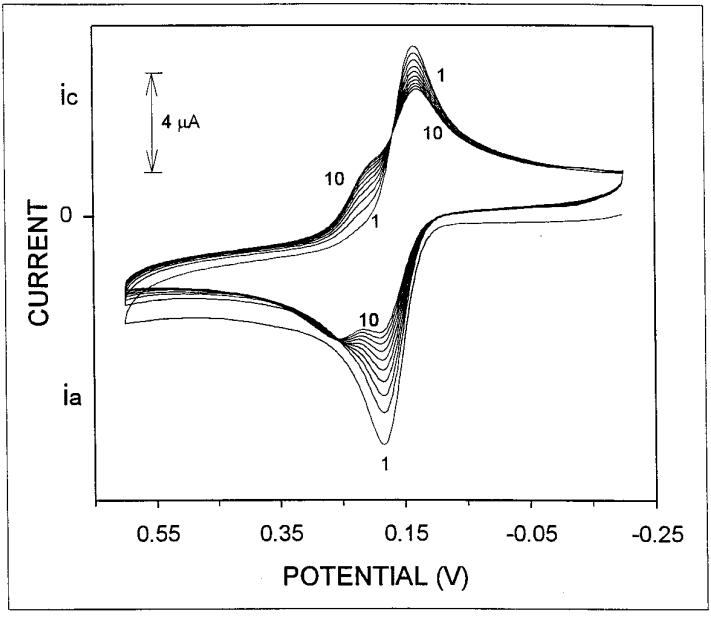

FIG. 6. Cyclic voltammogram of NBAD in the presence of NAcH in 0.1 M phosphate buffer at pH 7.0. The scan was initiated in the positive-going direction from −0.2 V at a rate of 100 mV/s. Concentrations of NBAD and NAcH were 0.3 and 400 mM, respectively.

for 0.3 mM NBAD quinone in 200 mM NAcH at pH 7.0 (Fig. 7), the absorbance at the λ_{max} of the quinone, 396 nm, decreases with time, indicating consumption of the quinone, whereas the absorbances at 244 and 284 nm increase with time, indicating the formation of a new product(s). The uv/vis spectra for 0.3 mM NBAD quinone in the presence of other concentrations of NAcH at pH 7.0 and for NBAD quinone of different concentrations in 200 mM NAcH at pH 7.0 were also recorded. All spectra show decreases in absorbance at 396 nm and increases in absorbances at 242 and 284 nm. The major product formed from the reaction of NBAD quinone with NAcH was determined to be an adduct of NBAD quinone with NAcH (*vide infra*). In addition, as seen in the NBAD quinone/imidazole system, a broad absorption from ca. 300 to 600 nm that is due to a minor unidentified product(s) is evident in the NBAD quinone/NAcH system (Table 2). Again, the relative yield of the unknown product(s) is related to the ratio of NAcH to NBAD quinone as well as the pH. Either a decrease in the ratio of NAcH to NBAD quinone or an increase in pH caused the relative yield of the unknown product(s) to increase.

Rate constants for the reaction of NBAD quinone with NAcH were estimated using the same procedures as those for the reactions of NADA quinone or NBAD quinone with imidazole (Table 2). Similar results were obtained. First, the results obtained for 0.15, 0.3, 0.6, and 0.9 mM NBAD quinone with 200 mM NAcH at pH 7.0 showed independence of the pseudo-first-order rate constant on quinone

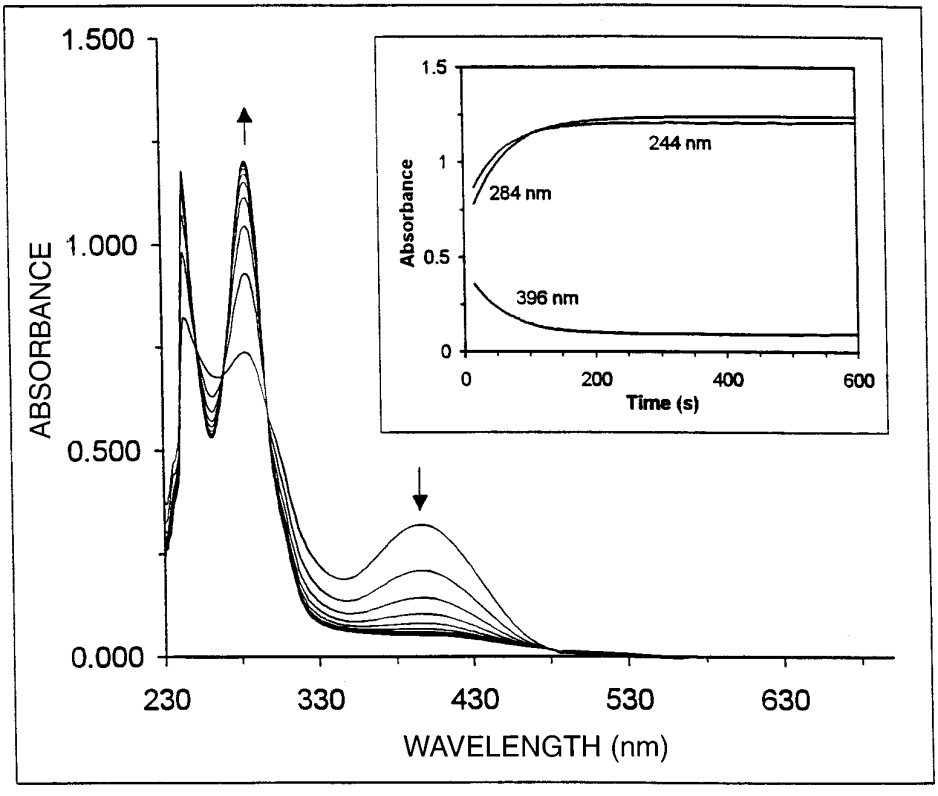

FIG. 7. Spectral changes associated with the reaction of 0.3 mM NBAD quinone with 200 mM NAcH at pH 7.0. Although spectral measurements were conducted at 15 s intervals from 15 to 600 s after mixing of NBAD quinone and NAcH solutions, for clarity only every other spectrum is shown here. (Inset) Absorbances at 244, 284, and 396 nm vs time.

concentration. Second, the results obtained for 0.3 mM NBAD quinone with 20, 50, 100, and 200 mM NAcH at pH 7.0 showed that the pseudo-first-order rate constants have a linear dependence on the concentration of NAcH (Fig. 8). The positive intercept is due to intrinsically slow reactions of NADA quinone or NBAD quinone with unidentified components of the solvent system. Third, since the pK_a of the conjugate acid of NAcH is 7.08, the equilibrium concentration of NAcH, which is the effective concentration of NAcH as a nucleophile, is only 45% of the analytical concentration of NAcH at pH 7.0. When the pseudo-first-order rate constants were divided by the equilibrium concentration of NAcH, an average value of 5.7×10^{-2} M^{-1} s^{-1} was obtained for the second-order rate constant (Table 2).

Liquid Chromatography of Product Mixture from Reaction of N-β-Alanyldopamine Quinone with N-Acetylhistidine

The composition of the product mixture obtained from mixing 90 μl of 1 mM NBAD quinone with 225 μl of 40 mM NAcH (1:100 molar ratio) at pH 7.0 was

TABLE 2
Rate Constants for NBAD Quinone/NAcH System

No.	[NBAD quinone] (mM)	C_{NAcH} (mM)[a]	pH	$[NAcH]_{eq}$ (mM)[b]	Pseudo-first-order rate const.[c] (s^{-1}) × 10^3	Second-order rate const.[d] (M^{-1} s^{-1}) × 10^2
1	0.15	200	7.0	90.8	4.7	5.2
2	0.30	200	7.0	90.8	4.9	5.4
3	0.60	200	7.0	90.8	4.6	5.1
4[e]	0.90	200	7.0	90.8	4.9	5.4
5[e]	0.30	20	7.0	9.1	0.7	7.3
6[e]	0.30	50	7.0	22.7	1.4	6.2
7	0.30	100	7.0	45.4	2.5	5.5

[a] C_{NAcH} is the analytical concentration of imidazole, i.e., the sum of the equilibrium concentrations of NAcH and its conjugate acid.

[b] $[NAcH]_{eq}$, the equilibrium concentration of NAcH, is calculated from the corresponding analytical concentration and pK_a of NAcH's conjugate acid, which is 7.08.

[c] The pseudo-first-order rate constants were obtained from slopes of plots for regression analyses of log(absorbance at 396 nm) vs time.

[d] The second-order rate constants were obtained by dividing the corresponding pseudo-first-order rate constants by the equilibrium concentrations of NAcH at the specified pH.

[e] In these cases, a broad absorption from ca. 300 to 600 nm is evident in the spectra of NBAD quinone in the presence of imidazole.

analyzed by LC with uv/vis and EC detection. The LC-EC (reduction) chromatogram showed no discernible peaks (data not shown), which indicates that the quinone had been consumed completely. In the corresponding LC-EC (oxidation) chromatogram there are three major peaks resolved (Fig. 9). The peak at 18.7 min is due to NBAD, whereas the peaks at 14.9 and 7.3 min are due to two reaction products, which are denoted here as NAcH–NBAD-I and NAcH–NBAD-II, respectively. Again, the amounts of the adducts and the catecholamine produced were related to the molar ratio of the initial concentrations of the quinone and imidazole. The [NAcH–NBAD-I and NAcH–NBAD-II]:[NBAD] ratios were approximately 3:1 and 7:1 when the [NBAD quinone]:[NAcH] ratios were 1:100 and 1:1000, respectively.

Identification and Characterization of N-Acetylhistidine Adducts of N-β-Alanyldopamine

In order to identify NAcH–NBAD-I and NAcH–NBAD-II, the adducts were synthesized and purified for structural analysis and characterization. Their molecular masses were determined by MALDI-MS. The results indicate that both are mono-addition adducts of NBAD (theoretical value: m/z = 420).

The structure of NAcH–NBAD-I was determined by NMR spectroscopic studies. For an ^1H NMR spectrum obtained in $H_2O:D_2O$ (90:10) at 30°C, the chemical shift assignments are as follows: δ (ppm) = 8.45 (s, 3H, NH13), 8.34 (s, 1H, H2′), 7.96 [s (br.), 1H, NH9], 7.94 (d, 1H, NH8′), 7.27 (s, 1H, H5′), 6.91 (s, 2H, H2, H5),

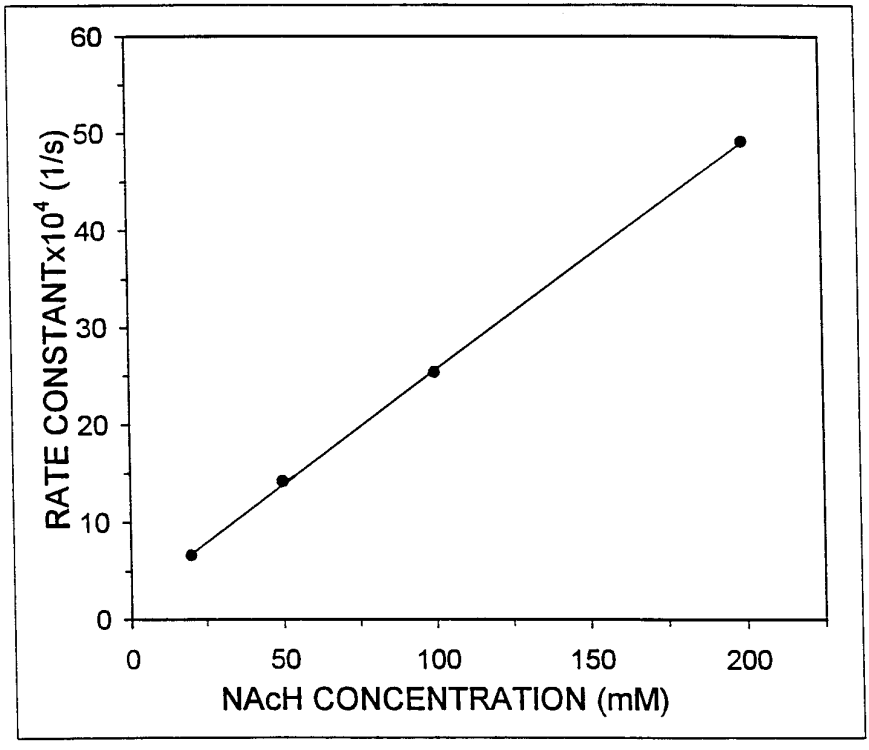

FIG. 8. The dependence of the rate constants for the reaction of NBAD quinone with NAcH on NAcH concentration at pH 7.0. The NBAD quinone concentration was 0.3 mM, whereas the analytical concentrations of NAcH were 20, 50, 100, and 200 mM, respectively. The pseudo-first-order rate constants were obtained from slopes of plots for regression analyses of log(absorbance at 396 nm) vs time.

4.45 (m, 1H, H7′), 3.23 (m, 1H, H6′a), 3.17 (m, 2H, H8), 3.16 (m, 2H, H12), 3.05 (m, 1H, H6′b), 2.56 (m, 2H, H11), 2.52 (m, 2H, H7), and 2.01 (s, 3H, H10′). These assignments were confirmed by two-dimensional heteronuclear multiple quantum coherence (HMQC) and total correlation spectroscopy (TOCSY) NMR experiments. The resonance signals of the two phenyl protons are overlapped at 6.91 ppm in the ^{1}H spectrum, but are more resolved in the HMQC spectrum. In order to resolve this overlapped signal in the ^{1}H NMR spectrum, a ^{1}H experiment was conducted in an alternative solvent containing acetone-d_6 and D_2O (10:1). The two phenyl protons exhibited two well-resolved singlets at 6.81 and 6.71 ppm (data not shown). Since neither *o*-coupling nor *m*-coupling is observed, the resonances of 6.91 ppm in H_2O/D_2O are assigned to H2 and H5. Therefore, NAcH–NBAD-I must be the C6 mono-addition adduct, 6-*N*-(*N*-acetylhistidyl)-*N*-β-alanyldopamine (6-NAcH–NBAD) (see Scheme 2 for structure).

The structure of NAcH–NBAD-II was also elucidated by ^{1}H NMR spectrometry. Several proton resonance peaks in the ^{1}H spectrum of this adduct are present in pairs, which may be due to a slow conformational change in the structure over the

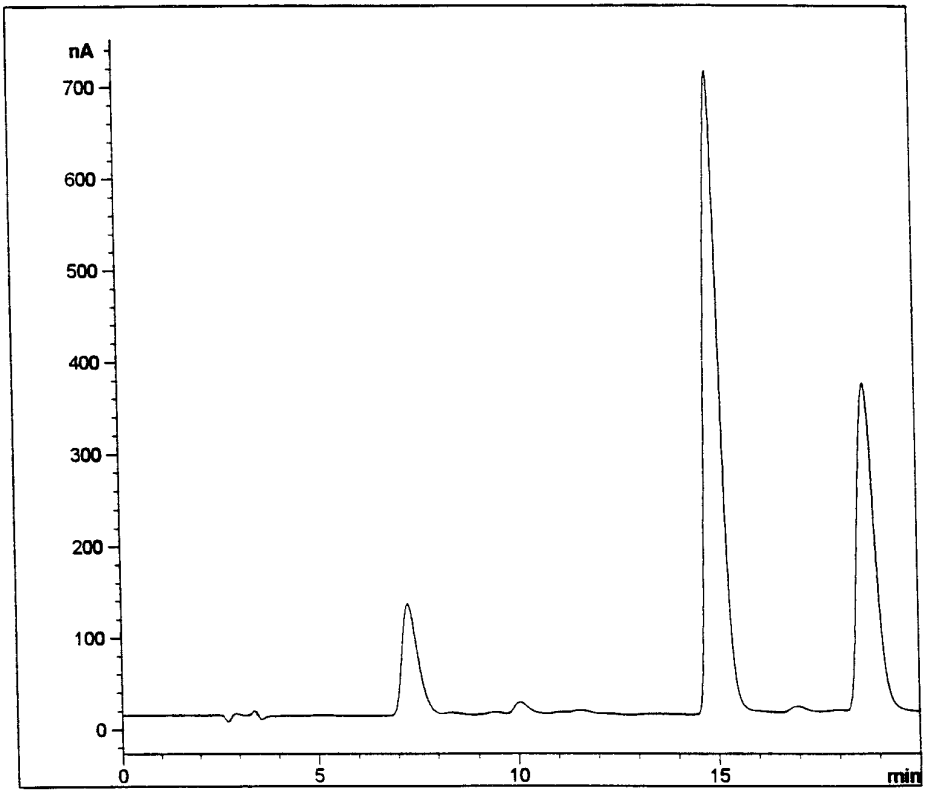

FIG. 9. LC-EC (oxidation) chromatogram of the product mixture from the reaction of NBAD quinone with NAcH (1:100 molar ratio) at pH 7.0.

NMR time scale. This feature and the pattern of the resonance signals are parallel to those of 2-NAcH–NADA (*28*). Therefore, NAcH–NBAD-II is assigned as the C2 monoaddition adduct, 2-*N*-(*N*-acetylhistidyl)-*N*-β-alanyldopamine (2-NAcH–NBAD). The chemical shift assignments are as follows: δ (ppm) = 8.41 (s, 1H, H2′), 7.22 and 7.18 (2s, 1H, H5′), 6.93 and 6.92 (2s, 1H, H5), 6.91 (s, 1H, H6), 4.22 and 4.16 [dd (J = 7.2, 4.9 Hz), dd (J = 8.4, 5.2 Hz), 2H, H7′], 3.30 and 3.22 (2m, 1H, H6′a), 3.15 (m, 2H, H8), 3.12 and 2.98 (2m, 2H, H12), 2.83 (m, 1H, H6′b), 2.54 (m, 1H, H7), 2.45 and 2.31 (2m, 2H, H11), and 1.90 and 1.87 (2s, 3H, H10′) (see Scheme 2 for structure).

The cyclic voltammetric behavior of adducts 6-NAcH–NBAD and 2-NAcH–NBAD in 0.1 M phosphate buffer at pH 7.0 was examined at a scan rate of 200 mV/s (Fig. 10). The results demonstrate that both adducts are oxidized at a more positive potential than NBAD and that the redox behavior of neither one is as electrochemically reversible as that of NBAD.

Ultraviolet/visible spectra of 6-NAcH–NBAD and 2-NAcH–NBAD were acquired during LC analysis of the product mixture from reactions of NBAD quinone

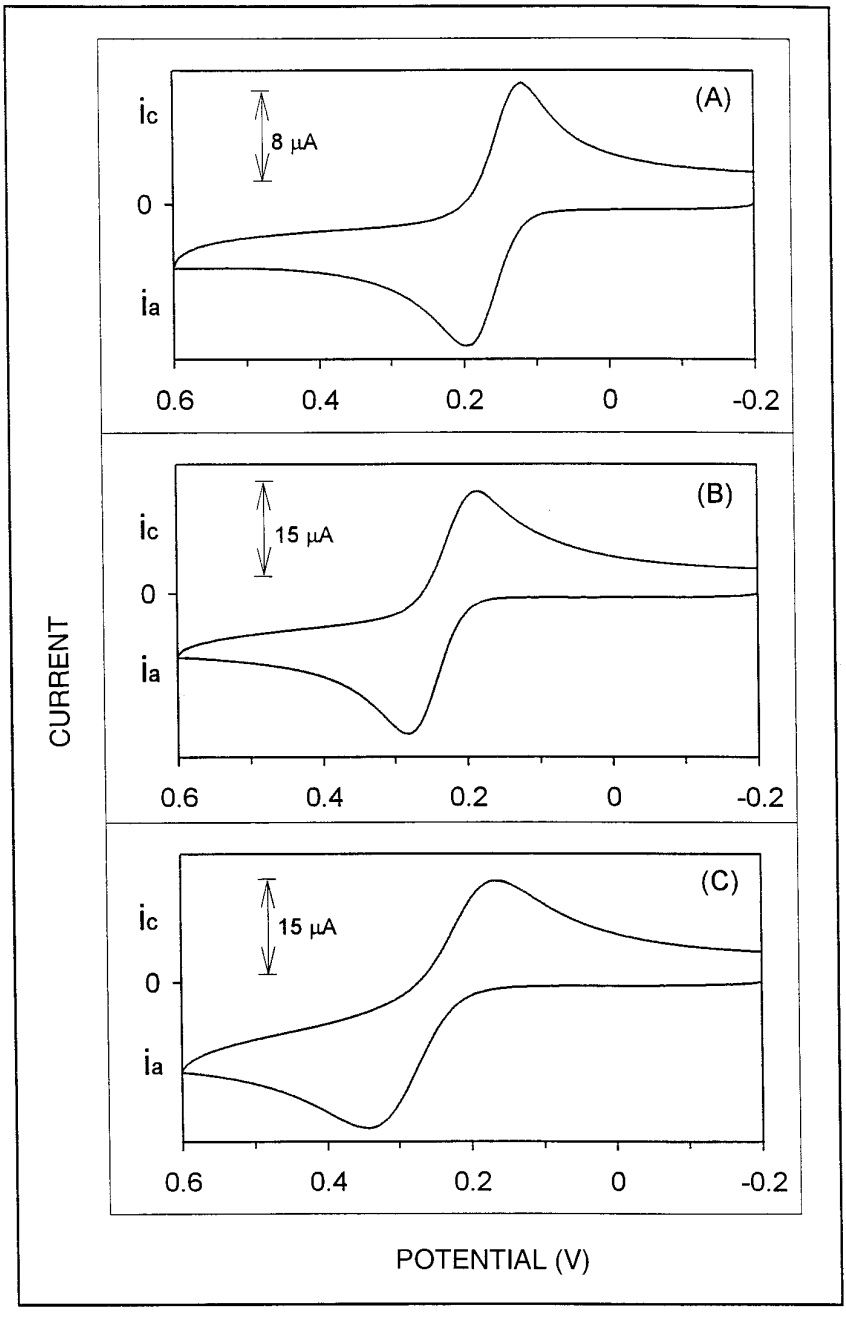

FIG. 10. Cyclic voltammograms of NBAD and its NAcH adducts in 0.1 M phosphate buffer at pH 7.0. The scan was initiated in the positive-going direction from −0.2 V at a rate of 200 mV/s. (A) NBAD, (B) 6-NAcH–NBAD, and (C) 2-NacH–NBAD.

with NAcH (data not shown). Both 6-NAcH–NBAD and 2-NAcH–NBAD have a uv λ_{max} at 284 nm. To estimate the relative molar ratio of the adducts 6-NAcH–NBAD and 2-NAcH–NBAD that formed during the reaction of NBAD with NAcH at a 1 : 100 molar ratio, a LC-UV chromatogram at 284 nm was obtained by extracting absorbances at 284 nm from the uv/vis spectra recorded during LC with on-line UV detection (data not shown). If the two monoaddition products are assumed to have equal molar absorption coefficients at 284 nm, then the relative molar ratio of 6-NAcH–NBAD to 2-NAcH–NBAD is estimated to be 6 : 1 on the basis of the areas of corresponding peaks in the LC-UV chromatogram.

DISCUSSION

Pathways for the nucleophilic additions of imidazole to NADA and NBAD quinones and for the nucleophilic additions of NAcH to NBAD are proposed in Scheme 2. Although imidazole and NAcH are both nitrogen-centered nucleophiles and yield the C6 adducts of NADA and NBAD as major products, imidazole does not yield the C2 adducts of NADA and NBAD in detectable amounts, whereas NAcH gives the C2 adducts as minor products. The ratios of the C6 to C2 NAcH adducts are approximately 7 : 1 for NADA quinone (*28*) and 6 : 1 for NBAD quinone when the [NAcH] : [NADA or NBAD quinone] ratio is 100.

The formation of a C2 NAcH adduct but not a C5 NAcH adduct with the quinone is intriguing. Both C2 and C5 of the quinone ring can be electrophilic reaction sites in Michael 1,6-addition reactions. However, C2 is expected to be less favored than C5, because the alkyl group at C1 is an electron-donating substituent that causes C2 to be less electropositive than C5. Also, the presence of the catecholamine side chain causes steric hinderance for nucleophilic attack at C2. We have no explanation for the regioselectivity of this addition reaction.

The reaction rates of imidazole with NADA and NBAD quinones are only slightly faster than those of NAcH. The uv/vis kinetics showed that the second-order rate constants for NADA quinone/imidazole, NBAD quinone/imidazole, and NBAD quinone/NAcH systems are 9.0×10^{-2}, 7.4×10^{-2}, and 5.7×10^{-2} M^{-1} s^{-1}, respectively (*vide supra*). If the equilibrium concentration of NAcH at pH 7 is taken into account, then the second-order rate constant for NADA quinone/NAcH system is 4.3×10^{-2} M^{-1} s^{-1} (*28*). The absence of the side chain of imidazole may account for its more rapid rate of reaction than NAcH. Based on these results, the rate of nucleophilic addition of histidyl residues of protein to catecholamine quinones would be expected to be slower than that of free NAcH, unless the protein has a special conformation to facilitate the reaction of one relative to the other.

The formation of 6-NAcH–NADA is consistent with a previous study in which NADA and NAcH were incubated with insect cuticle from late fifth instar larvae of *Hyalophora cecropia* (*19*). However, 2-NAcH–NADA, which was detected in our study as a minor product, was not identified in the cuticle-catalyzed coupling study (*19*). This observation might be because the C2 adduct either was present as one of the several unidentified products in the cuticle-catalyzed system or it was not formed under enzymatic conditions. The C2 position of the aromatic ring of

the quinones is more sterically hindered than C6, which is consistent with peak splitting in the NMR spectra of the 2-NAcH–NADA adduct. Moreover, in contrast to the results that are reported here, a side-chain product was detected when NADA and NAcH were incubated with insect cuticle (*18*). The absence of a side-chain adduct in our study indicates that nonenzymatic isomerization of the quinone to the quinone methide does not occur as rapidly as nucleophilic addition at ring carbons of the quinone. To our knowledge no adducts from reactions of NBAD quinone with amino acid derivatives have been previously characterized, although it was suggested in an earlier study in which NBAD and NACySH were incubated with insect cuticle that one of several unknown compounds resolved by chromatography was due to such an adduct (*5*).

Two types of side reactions of NADA and NBAD quinones have been observed. The first type involves formation of a minor product(s) that has a broad uv/vis absorption in the range of 300 to 600 nm (Fig. 4). The second side reaction is the reduction of quinones by an unknown reductant to regenerate NADA and NBAD, as demonstrated by results of LC (Figs. 5 and 9). Both side reactions also are observed for NADA or NBAD quinones in buffer solutions in the absence of nucleophiles (unpublished data), but they are suppressed when other more reactive nucleophiles are present. These results indicate that there is competition for the quinones between nucleophilic addition reactions and side reactions. One possible side reaction is addition of a component of the solvent/buffer system such as water to the quinone to generate a catecholamine adduct that is more easily oxidized than the original catecholamine. If this reaction were to occur, then unreacted quinone would become involved in a redox reaction and reduced to the original catecholamine.

In conclusion, this study has delineated the reactions of NADA and NBAD quinones with the nitrogen-centered nucleophiles, imidazole and NAcH. Together with results from the recent structural elucidation of four natural cross-links in the insect exoskeleton (*22*), these data provide definitive evidence for the participation of histidyl residues of cuticular protein in the sclerotization of the insect exoskeleton and are consistent with the previously obtained solid-state NMR results that indicated the presence of C–N linkages in cuticle but did not reveal the exact structures (*14*). The reactions of NADA with NAcH in the presence of cuticle were previously found to yield C6 and C7 adducts (*18*, *20*). However, we have shown that nucleophilic additions at C2 of the catecholamine quinones by NAcH also occur. No formation of side-chain adducts occurs in our model systems, indicating that spontaneous quinone isomerization is not favored in the absence of an appropriate enzymatic system. The kinetics for the reactions of NADA and NBAD quinone with the two nucleophiles were obtained for the first time, which provide information about the rates of reactions between sclerotizing agents and histidyl groups in cuticular proteins.

ACKNOWLEDGMENTS

The authors extend thanks to Dr. Kenneth Tomer, Dr. Todd Williams, and Mr. Gary Radke for their assistance in mass spectrometry and Dr. Om Prakash for his assistance in NMR spectroscopy. We also thank Dr. T. L. Hopkins, Dr. Maryanne Collinson, and Mr. T. Morgan for assistance with this study

and for reviewing the manuscript. This research was supported in part by National Science Foundation Grants DCB-9019400, MCB-9418129, and CHE-9216101.

REFERENCES

1. Hopkins, T. L., and Kramer, K. J. (1992) *Annu. Rev. Entomol.* **37,** 273–302.
2. Andersen, S. O., Peter, M. G., and Roepstorff, P. (1996) *Comp. Biochem. Physiol.* **113B,** 689–705.
3. Pryor, M. G. M. (1940a) *Proc. R. Soc. London Ser. B* **128,** 378–393.
4. Pryor, M. G. M. (1940b) *Proc. R. Soc. London Ser. B* **128,** 393–407.
5. Sugumaran, M., Saul, S. J., and Dali, H. (1990) *Arch. Insect Biochem. Physiol.* **15,** 255–269.
6. Sugumaran, M. (1988) *Adv. Insect Physiol.* **21,** 179–231.
7. Ricketts, D., and Sugumaran, M. (1994). *J. Biol. Chem.* **269,** 22217–22221.
8. Hackman, R. H., and Goldberg, M. (1977) *Insect Biochem.* **7,** 175–184.
9. Karlson, P, and Sekeris, C. E. (1962) *Nature* **195,** 183–184.
10. Andersen, S. O. (1971) *Insect Biochem.* **1,** 157–170.
11. Hopkins, T. L., Morgan, T. D., Aso, Y., and Kramer, K. J. (1982) *Science* **217,** 364–366.
12. Hopkins, T. L., Morgan, T. D., and Kramer, K. J. (1984) *Insect Biochem.* **14,** 533–540.
13. Sugumaran, M., and Lipke, H. (1982) *Proc. Natl. Acad. Sci. USA* **79,** 2480–2484.
14. Schaefer, J., Kramer, K. J., Garbow, J. R., Jacob, G. S., Stejskal, E. O., Hopkins, T. L., and Speirs, R. D. (1987) *Science* **235,** 1200–1204.
15. Christensen, A. M., Schaefer, J., Kramer, K. J., Morgan, T. D., and Hopkins, T. L. (1991a) *J. Am. Chem. Soc.* **113,** 6799–6802.
16. Christensen, A. M., Schaefer, J., and Kramer, K. J. (1991b). *Magn. Reson. Chem.* **29,** 418–421.
17. Kramer, K. J., and Hopkins, T. L. (1995) *Insect Biochem. Mol. Biol.* **25,** 1067–1080.
18. Andersen, S. O., Jacobsen, J. P., Roepstorff, P., and Peter, M. G. (1991) *Tetrahedron Lett.* **32,** 4287–4290.
19. Andersen, S. O., Peter, M. G., and Roepstorff, P. (1992a) *Insect Biochem. Mol. Biol.* **22,** 459–469.
20. Andersen, S. O., Jacobsen, J. P., and Roepstorff, P. (1992b) *Insect Biochem. Mol. Biol.* **22,** 517–527.
21. Wybrandt, G. B., and Andersen, S. O. (1994) *Biochim. Biophys. Acta* **1201,** 15–18.
22. Xu, R., Huang, X., Hopkins, T. L., Kramer, K. J. (1997) *Insect Biochem. Mol. Biol.* **27,** 101–108.
23. Andersen, S. O. (1980) *in* Cuticle Techniques in Arthropods (Miller, T. A., Ed.), pp. 200–201, Springer-Verlag, New York.
24. Kramer, K. J., Nuntnarumit, C., Aso, Y., Hawley, M. D., and Hopkins, T. L. (1983) *Insect Biochem.* **13,** 475–479.
25. Yamasaki, N., Aso, Y., and Tsukamoto, T. (1990) *Agric. Biol. Chem.* **54,** 833.
26. Van Swaay, M. (1978) *J. Chem. Ed.* **55,** A7–A12.
27. Huang, X. (1996) Ph.D. Dissertation, Kansas State University, Manhattan.
28. Xu, R., Huang, X., Morgan, T. D., Prakash, O., Kramer, K. J., and Hawley, M. D. (1996) *Arch. Biochem. Biophys.* **329,** 56–64.
29. Xu, R., Huang, X., Kramer, K. J., and Hawley, M. D. (1995) *Anal. Biochem.* **231,** 72–81.